Advanced Structured Materials

Holm Altenbach · Joël Pouget
Martine Rousseau · Bernard Collet
Thomas Michelitsch *Editors*

Generalized Models and Non-classical Approaches in Complex Materials 2

Springer

Holm Altenbach · Joël Pouget
Martine Rousseau · Bernard Collet
Thomas Michelitsch
Editors

Generalized Models and Non-classical Approaches in Complex Materials 2

Springer

Editors
Holm Altenbach
Institut für Mechanik
Otto-von-Guericke-Universität Magdeburg
Magdeburg
Germany

Joël Pouget
Centre National de la Recherche
Scientifique, UMR 7190,
Institut Jean Le Rond d'Alembert
Sorbonne Université
Paris
France

Martine Rousseau
Centre National de la Recherche
Scientifique, UMR 7190,
Institut Jean Le Rond d'Alembert
Sorbonne Université
Paris
France

Bernard Collet
Centre National de la Recherche
Scientifique, UMR 7190,
Institut Jean Le Rond d'Alembert
Sorbonne Université
Paris
France

Thomas Michelitsch
Centre National de la Recherche
Scientifique, UMR 7190,
Institut Jean Le Rond d'Alembert
Sorbonne Université
Paris
France

ISSN 1869-8433 ISSN 1869-8441 (electronic)
Advanced Structured Materials
ISBN 978-3-319-77503-6 ISBN 978-3-319-77504-3 (eBook)
https://doi.org/10.1007/978-3-319-77504-3

Library of Congress Control Number: 2018934438

Printed on acid-free paper

This Springer imprint is published by the registered company Springer International Publishing AG part of Springer Nature
The registered company address is: Gewerbestrasse 11, 6330 Cham, Switzerland

Dedicated to the memory of a great creative spirit, G. A. Maugin

Chapter 6
Emulating the Raman Physics in the Spatial Domain with the Help of the Zakharov's Systems

Evgeny M. Gromov and Boris A. Malomed

Abstract Dynamics of solitons is considered in the framework of the extended nonlinear Schrödinger equation (NLSE), which is derived from a system of the Zakharov's type for the interaction between high- and low-frequency (HF and LF) waves, in which the LF field is subject to diffusive damping. The model may apply to the propagation of HF waves in plasmas. The resulting NLSE includes a *pseudo-stimulated-Raman-scattering* (pseudo-SRS) term, i.e., a spatial-domain counterpart of the SRS term which is well known as an ingredient of the temporal-domain NLSE in optics. Also included is inhomogeneity of the spatial second-order diffraction (SOD). It is shown that the wavenumber downshift of solitons, caused by the pseudo-SRS, may be compensated by an upshift provided by the SOD whose coefficient is a linear function of the coordinate. An analytical solution for solitons is obtained in an approximate form. Analytical and numerical results agree well, including the predicted balance between the pseudo-SRS and the linearly inhomogeneous SOD.

6.1 Introduction

The great interest to the dynamics of solitons is motivated by their ability to travel long distances keeping the shape and transferring the energy and information with no or little loss. Soliton solutions are relevant to nonlinear models in various areas

E. M. Gromov (✉)
National Research University Higher School of Economics, Nizhny Novgorod 603155, Russia
e-mail: egromov@hse.ru

B. A. Malomed
Faculty of Engineering, Department of Physical Electronics, Tel Aviv University, 69978 Tel Aviv, Israel
e-mail: malomed@post.tau.ac.il

B. A. Malomed
ITMO University, St. Petersburg 197101, Russia

H. Altenbach et al. (eds.), *Generalized Models and Non-classical Approaches in Complex Materials 2*, Advanced Structured Materials 90,
https://doi.org/10.1007/978-3-319-77504-3_6

of physics which deal with the propagation of intensive wave fields in dispersive media: optical pulses and beams in fibers and spatial waveguides, electromagnetic waves in plasma, surface waves (SW) on deep water, etc. [1–7]. Recently, solitons have also drawn a great deal of interest in plasmonics [8–10].

The propagation of broad high-frequency (HF) wave packets is modeled by the second-order nonlinear dispersive wave theory. In isotropic media, the basic equation of the theory is the nonlinear Schrödinger equation (NLSE) [11, 12], which combines the second-order dispersion (SOD) and the self-phase modulation. Its soliton solutions provide for the equilibrium of the dispersive dilatation and nonlinear compression of the wave packets. In particular, permanent-shape solutions for damped solitons were found in the framework of the NLSE including linear losses of HF waves and spatially-decreasing SOD [4, 13].

In anisotropic media, the copropagation of wave modes with different polarizations gives rise to coupled NLSEs [14–17], which include cross-phase-modulation (XPM) terms. Interactions of vector solitons in the framework of coupled NLSEs were studied in detail too, see, e.g., [18–20].

The dynamics of narrow HF wave packets is described by the third-order nonlinear dispersive wave theory [1], which takes into account the nonlinear dispersion (self-steeping) [21], stimulated Raman scattering (SRS) [22–24] and third-order dispersion (TOD). In isotropic media the basic equation of the theory is the third-order NLSE [24–28]. Soliton solutions in the framework of the third-order NLSE with TOD and nonlinear dispersion were found in Refs. [29–36]. In Refs. [37, 38], stationary kink waves were found as solutions of the extended NLSE with SRS and nonlinear dispersion terms. This solution exists as the equilibrium between the nonlinear dispersion and SRS. For localized nonlinear wave packets (solitons), the SRS gives rise to the downshift of the soliton spectrum [22–24] and eventually to destabilization of the solitons. The use of the balance between the SRS and the slope of the gain for the stabilization of solitons in long telecom links was proposed in [25]. The compensation of the SRS by emission of linear radiation fields from the soliton's core was considered in [26]. In addition, the compensation of the SRS in inhomogeneous media was considered in several situations, viz., with periodic SOD [27, 28], shifted zero-dispersion point of SOD [29], and in dispersion-decreasing fibers [30].

In anisotropic media the dynamics of narrow vector wave packets is described by coupled third-order NLSEs, which take into account third-order cross-nonlinear terms [31–34]. In the framework of this system, which does not include SRS terms, vector-soliton solutions were found in [32]. Interactions of vector solitons in the framework of coupled third-order NLSEs were considered in [35].

Intensive short pulses of HF electromagnetic or Langmuir wave in plasmas, as well as HF SW in deep stratified water, suffer effective induced damping due to scattering on LF waves, which, in turn, are subject to the action of viscosity. These LF modes are ion-sound waves in the plasma, and internal waves (IW) in the stratified fluid. The first model for the damping induced by the interaction with the LF waves was proposed in [35] (see Sect. 6.2). This model gives rise to an extended NLSE with the spatial-domain counterpart of the SRS term, that was call a

pseudo-SRS one (*pseudo-Raman*). The equation was derived from the system of the Zakharov's type equations [37, 38] for the coupled Langmuir and ion-acoustic waves in plasmas. The pseudo-SRS leads to the self-wavenumber downshift, similar to what is well known in the temporal domain [1, 21–24] and, eventually, to destabilization of the solitons. The model elaborated in [36] also included smooth spatial variation of the SOD, accounted for by a spatially decreasing SOD coefficient, which leads to an increase of the soliton's wavenumber, making it possible to compensate the effect of the pseudo-SRS on the soliton by the spatially inhomogeneous SOD, neglecting the direct effect of the LF-wave loss.

The objective of this article is to produce a review of models derived, starting from systems of the Zakharov's type, in the form of NLSEs which include the pseudo-Raman term and other terms which produce soliton pulses as a result of competition with the pseudo-Raman effect. After reviewing the basic model equation in Sect. 6.2, in Sect. 6.3 we consider the dynamics of intensive HF wave packets in dispersive nonlinear media, taking into account the scattering on the damped LF waves (pseudo-Raman), exponentially decreasing SOD, and linear losses of HF waves [39].

In Sect. 6.4 the soliton dynamics is considered in the framework of an higher-order NLSE with a pseudo-Raman effect, decreasing SOD, taking into account nonlinear dispersion and TOD too [40]. The equilibrium between the pseudo-SRS and decreasing SOD is considered. The equilibrium state is a stable focus for negative nonlinear dispersion and positive TOD, and an unstable focus for positive nonlinear dispersion and negative TOD.

In Sect. 6.5 we address the dynamics of vector solitons in the framework of coupled extended NLSEs, taking into account pseudo-Raman, cross-pseudo-SRS, XPM and inhomogeneous SOD [41]. Using analytical and numerical methods, the compensation of the soliton's Raman self-wavenumber downshift by the upshift caused by the decreasing SOD is shown. An analytical vector-soliton solution is found in the framework of coupled extended NLSEs, representing the equilibrium of pseudo-SRS and inhomogeneous SOD. The soliton exists with an additional wavenumber lower than a certain critical value, which is proportional to the amplitude of the wave packet. By means of direct simulations, we also address evolution initiated by an input with spatially even and odd components, which reveals different outcomes, depending on the value of the relative amplitude of the two components.

In Sect. 6.6 dynamics of solitons is considered in the framework of an extended nonlinear NLSE, which is derived from a Zakharov-type model for wind-driven HF SW in the ocean, coupled to damped LF IW [42]. The drive gives rise to a convective (but not absolute) instability in the system. The resulting NLSE includes a pseudo-SRS term, which is a spatial-domain counterpart of the SRS term. Analysis of the field-momentum balance and direct simulations demonstrate that wavenumber downshift by the pseudo-SRS may be compensated by the upshift induced by the wind traction, thus maintaining robust bright solitons in both stationary and oscillatory forms; in particular, they are not destroyed by the underlying convective instability.

6.2 Soliton Dynamics in an Extended Nonlinear Schrödinger Equation with a Pseudo-Raman Effect and Inhomogeneous Dispersion

We consider the evolution of slowly varying envelope $U(\xi, t)$ of the intense HF wave field in the nonlinear medium with inhomogeneous SOD, taking into account the interaction with LF variations of the medium's parameter $n(\xi, t)$ (such as the refractive index in optics), which suffers the action of effective diffusion. The unidirectional propagation of the fields along coordinate ξ is described by the system of the Zakharov's type [37, 38]:

$$2i\frac{\partial U}{\partial t} + \frac{\partial}{\partial \xi}\left(q(\xi)\frac{\partial U}{\partial \xi}\right) - nU = 0, \tag{6.1}$$

$$\frac{\partial n}{\partial t} + \frac{\partial n}{\partial \xi} - \mu\frac{\partial^2 n}{\partial \xi^2} = -\frac{\partial |U|^2}{\partial \xi}, \tag{6.2}$$

where μ is the diffusion coefficient. In particular, this system may describe intense electromagnetic or Langmuir waves in plasmas, taking into account the scattering on ion-acoustic waves, which are subject to the viscous damping. In the third-order approximation of the theory (for short HF wave packets, with $k\Delta \ll \mu$, where k and Δ are the spatial extension and characteristic wave number of the wave packet), Eq. (6.2) may approximated by the nonlinear response of the medium, $n = -|U|^2 - \mu\partial\left(|U|^2\right)/\partial\xi$, which leads to the following extended NLSE for the HF amplitude:

$$2i\frac{\partial U}{\partial t} + \frac{\partial}{\partial \xi}\left[q(\xi)\frac{\partial U}{\partial \xi}\right] + 2\alpha U|U|^2 + \mu U\frac{\partial\left(|U|^2\right)}{\partial \xi} = 0, \tag{6.3}$$

where $\alpha = 1/2$. Below, we fix $\alpha = 1$ by means of obvious scaling. The last term in Eq. (6.3) represents the above-mentioned pseudo-Raman effect in the spatial domain.

Equation (6.3) with zero boundary conditions at infinity, $U|_{\xi\to\pm\infty} \to 0$, gives rise to the following integral relations for field moments, which will be used below:

$$\frac{dN}{dt} \equiv \frac{d}{dt}\int_{-\infty}^{+\infty} |U|^2 d\xi = 0, \tag{6.4}$$

$$2\frac{d}{dt}\int_{-\infty}^{+\infty} K|U|^2 d\xi = -\mu \int_{-\infty}^{\infty} \left[\frac{\partial\left(|U|^2\right)}{\partial\xi}\right]^2 d\xi - \int_{-\infty}^{\infty} \frac{dq}{d\xi}\left|\frac{\partial U}{\partial\xi}\right|^2 d\xi, \tag{6.5}$$

$$\frac{d}{dt}\int_{-\infty}^{+\infty} \xi|U|^2 d\xi = \int_{-\infty}^{+\infty} qK|U|^2 d\xi, \tag{6.6}$$

where the complex field is represented as $U \equiv |U|\exp(i\phi)$, and $K \equiv \partial\phi/\partial\xi$ is the local wavenumber.

For the analytical consideration of the wave-packet dynamics, we assume that scale of the inhomogeneity of the SOD term is much larger than the spatial width of the wave-packet envelope, $D_q \gg D_{|U|}$. Then, a solution of system (6.5)–(6.6) may be obtained in the adiabatic approximation, based on the use of the sech-like ansatz:

$$U(\xi,t) = A(t)\mathrm{sech}\left[\frac{\xi-\bar{\xi}(t)}{\Delta(t)}\right]\exp\left[ik(t)\xi - i\int \Omega(t)dt\right], \tag{6.7}$$

where $\Delta(t) = \sqrt{q(\bar{\xi})}/A(t), \Omega(t) = A^2(t)/2, A^2(t)\Delta(t) = \mathrm{const}, \bar{\xi}(t) = N^{-1}\int_{-\infty}^{+\infty}\xi|U|^2 d\xi$. Substituting (6.7) in (6.5)–(6.6) we derive a system of evolution equations the system for free parameters k and $\bar{\xi}$:

$$2\frac{dk}{dt} = -\frac{8}{15}\frac{\mu A_0^4 q_0^2}{q^3(\bar{\xi})} - \frac{q'(\bar{\xi})A_0^2 q_0}{3q^2(\bar{\xi})} - q'(\bar{\xi})k^2,\ \frac{d\bar{\xi}}{dt} = kq(\bar{\xi}), \tag{6.8}$$

where initial values are $q_0 \equiv q\left(\bar{\xi}(t=0)\right), A_0 \equiv A(t=0)$, which obey the above-mention relation, $A^2(t)q\left(\bar{\xi}(t)\right) = A^2(t=0)q\left(\bar{\xi}(t=0)\right) \equiv A_0^2 q_0$, and $q'\left(\bar{\xi}\right) \equiv dq/d\xi|_{\xi=\bar{\xi}}$ is the derivative (*slope*) of the SOD coefficient at the soliton's center. Equation (6.8) give rise to an obvious equilibrium state (alias a fixed point, FP):

$$8\mu q_0 A_0^2 = -5q'(\bar{\xi}_*)q(\bar{\xi}_*), k_* = 0, \tag{6.9}$$

where $\bar{\xi}_*$ is the equilibrium position of the soliton. For $\mu = \mu_* \equiv -(5/8)q'(\bar{\xi}_0)/A_0^2$ the equilibrium position of the soliton coincides with its initial position, $\bar{\xi}_* = \bar{\xi}_0 \equiv \bar{\xi}(t=0)$. For $\mu \neq \mu_*$ soliton's parameters are time-varying. To analyze the evolution around the FP, we assume linearly decreasing SOD, $q' = \mathrm{const} < 0$, and rescale the variables by defining $\tau \equiv -tq'A_0/\sqrt{3q_0}$,

$$y(\tau) \equiv k(\tau)\sqrt{3q_0}/A_0, n(\tau) = q\left(\bar{\xi}(\tau)\right)/q_0. \tag{6.10}$$

Then system (6.8) is reduced to

$$2\frac{dy}{d\tau} = -\frac{\lambda}{n^3} + \frac{1}{n^2} + y^2, \quad \frac{dn}{d\tau} = -ny, \tag{6.11}$$

where $\lambda \equiv -8\mu A_0^2/\left(5q'\right) \equiv \mu/\mu_*$. The first integral of Eq. (6.11) is

$$2y^2n^3 - \left(2y_0^2 + \lambda - 2\right)n^2 - 2n + \lambda = 0, \tag{6.12}$$

where $y_0 = y(\tau = 0)$. Dynamical invariant (6.12) is drawn in the plane of (y, n) in Fig. 6.1a, for $y_0 = 0$ and different values of λ. Trajectories in the plot are closed for $0 < \lambda < 2$, and open otherwise.

Further, at $y_0^2 > 0$ straightforward analysis of Eq. (6.11) demonstrates that the closed trajectories, which are shown in Fig. 6.1a for $y_0^2 = 0$, stretch in both positive and negative vertical directions (along the axis of n). In the same case, the critical value of the pseudo-SRS coefficient, which leads to the destruction of the soliton, decreases to $\lambda_{\rm cr} = 2\left(1 - y_0^2\right)$, the destruction being signaled by the disappearance of closed trajectories. Thus, the solitons do not exist at $y_0^2 > 1$; in other words, they exist with the wavenumber smaller than a critical value, $k^2 < A_0^2\alpha/(3q_0)$. Contours of dynamical invariant (6.12) are plotted in the plane of (y, n) in Fig. 6.1b, for $0 < y_0^2 < 1$ and several values of λ.

We look for stationary solutions to Eq. (6.3), where the SOD with linear spatial profile is adopted, in the form of a stationary wave profile, $U(\xi, t) = \psi(\xi)\exp(i\Omega t)$:

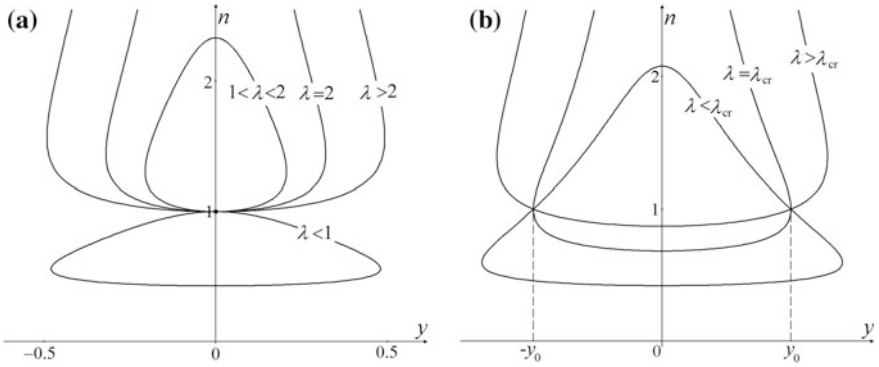

Fig. 6.1 Contour plots of dynamical invariant (6.12) in the plane of (y, n) of the soliton's rescaled dispersion and wavenumber (see Eq. (6.10)) for $y_0 = 0$ (**a**) and $0 < y_0^2 < 1$ (**b**), and different values of constant λ

$$\left(q_0 + q'\xi\right)\frac{d^2\psi}{d\xi^2} + q'\frac{d\psi}{d\xi} + 2\psi^3 - 2\Omega\psi + \mu\psi\frac{d(\psi^2)}{d\xi} = 0. \tag{6.13}$$

Next, with regard to the underlying assumption that the soliton's width is much smaller than the scale of the spatial inhomogeneity for the SOD, a solution to Eq. (6.13) is found in the form of $\psi = \psi_0 + \psi_1$, where ψ_1 is a small correction produced by terms $\sim q'$ and $\sim \mu$ in Eq. (6.13). In this approximation, we obtain

$$q_0\frac{d^2\psi_0}{d\xi^2} + 2\psi_0^3 - 2\Omega\psi_0 = 0, \tag{6.14}$$

$$q_0\frac{d^2\psi_1}{d\xi^2} + \left(6\psi_0^2 - 2\Omega\right)\psi_1 = -q'\frac{d^2\psi_0}{d\xi^2}\xi - \frac{2}{3}\mu\frac{d\left(\psi_0^3\right)}{d\xi} - q'\frac{d\psi_0}{d\xi}. \tag{6.15}$$

Equation (6.14) gives rise to the classical soliton solution, $\psi_0 = A_0\mathrm{sech}(\xi/\Delta)$, where $\Delta \equiv \sqrt{q_0}/A_0$ and $\Omega \equiv A_0^2/2$. Then substitutions $\eta = \xi/\Delta$ and $\Psi = \psi_1 q_0/\left(A_0 q_\eta'\right)$ cast Eq. (6.15) in the form of

$$\frac{d^2\Psi}{d\eta^2} + \left(\frac{6}{\cosh^2\eta} - 1\right)\Psi = \frac{\eta}{\cosh\eta} - \frac{2\eta}{\cosh^3\eta} - \frac{5}{4}\frac{\mu}{\mu_*}\frac{\sinh\eta}{\cosh^4\eta} + \frac{\sinh\eta}{\cosh^2\eta}, \tag{6.16}$$

where the equilibrium value of the pseudo-SRS coefficient is $\mu_* \equiv -5q'/(8A_0)$. For $\mu = \mu_*$ Eq. (6.16) has an *exact* localized solution for the correction to the standard sech soliton,

$$\Psi(\eta) = (1/4)\tanh\eta(\mathrm{sech}\eta)\left[\eta^2 - \ln(\cosh\eta)\right], \tag{6.17}$$

cf. a similar solution reported by [43]. It satisfies boundary conditions $\Psi(\eta \to \pm\infty) \to 0$. This spatially antisymmetric solution exists due to the balance between the pseudo-SRS term and linearly decreasing SOD.

6.3 Damped Solitons in an Extended Nonlinear Schrödinger Equation with a Pseudo-Raman Effect and Exponentially Decreasing Dispersion

We consider the evolution of a slowly varying envelope, $U(\xi, t)$, of the intensive HF wave field in the nonlinear medium with inhomogeneous SOD, taking into account the interaction with the damped LF wave, which is represented by the local perturbation of the effective refractive index, $n(\xi, t)$. The respective system of the

Zakharov's type for the unidirectional propagation of the HF and LF waves is [37, 38]

$$2i\left(\frac{\partial U}{\partial t}+V\frac{\partial U}{\partial x}\right)+\frac{\partial}{\partial x}\left[q(x)\frac{\partial U}{\partial x}\right]-nU+i\nu U=0, \tag{6.18}$$

$$\frac{\partial n}{\partial t}+V_S\frac{\partial n}{\partial x}-\delta\frac{\partial^2 n}{\partial x^2}=-\frac{\partial\left(|U|^2\right)}{\partial x}, \tag{6.19}$$

where ν is the linear-losses coefficient of the HF waves, δ is the viscosity of the LF waves, V is the HF group velocity, and V_S is the velocity of LF waves. As mentioned above, this system may describe intensive Langmuir waves in isotropic plasmas coupled to ion-sound waves, which are subject to the viscous damping.

In the third-order approximation of the theory (see Sect. 6.2) system (6.18)–(6.19) leads to the following evolution equation for the HF envelope amplitude:

$$2i\frac{\partial U}{\partial t}+\frac{\partial}{\partial\xi}\left[q(\xi+Vt)\frac{\partial U}{\partial\xi}\right]+2\alpha U|U|^2+\mu U\frac{\partial\left(|U|^2\right)}{\partial\xi}+i\nu U=0, \tag{6.20}$$

where $\xi=x-Vt$, term $\mu U\partial\left(|U|^2\right)/\partial\xi$, with $\mu\equiv\delta(V_S-V)^{-2}$, is, as above, the spatial counterpart of the SRS effect in the temporal domain, and $\alpha\equiv(1/2)(V_S-V)^{-1}$. Below, we fix $\alpha=1$ by means of obvious scaling. After the substitution of $U\equiv W\exp(-\nu t/2)$, Eq. (6.3) takes the form of

$$2i\frac{\partial W}{\partial t}+\frac{\partial}{\partial\xi}\left[q(\xi+Vt)\frac{\partial W}{\partial\xi}\right]+2W|W|^2\exp(-\nu t)+\mu W\frac{\partial\left(|W|^2\right)}{\partial\xi}\exp(-\nu t)=0. \tag{6.21}$$

Equation (6.21) with zero boundary conditions at infinity, $W|_{\xi\to\pm\infty}\to 0$, gives rise to the following integral relations for the field moments:

$$\frac{dN}{dt}\equiv\frac{d}{dt}\int_{-\infty}^{+\infty}|W|^2d\xi=0, \tag{6.22}$$

$$2\frac{d}{dt}\int_{-\infty}^{+\infty}K|W|^2d\xi=-\mu\exp(-\nu t)\int_{-\infty}^{\infty}\left[\frac{\partial\left(|W|^2\right)}{\partial\xi}\right]^2d\xi-\int_{-\infty}^{\infty}\frac{\partial q}{\partial\xi}\left|\frac{\partial W}{\partial\xi}\right|^2d\xi, \tag{6.23}$$

$$\frac{d}{dt}\int_{-\infty}^{\infty}\xi|W|^2d\xi=\int_{-\infty}^{+\infty}qK|W|^2d\xi. \tag{6.24}$$

For the analytical consideration of the wave-packet dynamics, we again assume that the scale of the inhomogeneity of the SOD term is much larger than the spatial width of the wave-packet envelope, $D_q \gg D_{|W|}$.

We take the HF wave packet as

$$W(\xi,t)=A(t)\mathrm{sech}\left[\frac{\xi-\overline{\xi}(t)}{\Delta(t)}\right]\exp\left[ik(t)\xi-i\int\Omega(t)dt\right], \tag{6.25}$$

cf. Eq. (6.7), where $\Delta(t)=\sqrt{q\left(\overline{\xi}+Vt\right)}/\left(A(t)\sqrt{\exp(-\nu t)}\right), \Omega(t)=A^2(t)\exp(-\nu t)/2, A^2(t)\Delta(t)=\text{const}$, $\overline{\xi}(t)=N^{-1}\int_{-\infty}^{+\infty}\xi|U|^2d\xi$. Substituting (6.25) in (6.23)–(6.24), we derive the dynamical system:

$$2\frac{dk}{dt}=-\frac{8}{15}\frac{\mu A_0^4\exp(-4\nu t)q_0^2}{q^3\left(\overline{\xi}+Vt\right)}-\frac{q'\left(\overline{\xi}+Vt\right)A_0^2\exp(-2\nu t)q_0}{3q^2\left(\overline{\xi}+Vt\right)}-q'\left(\overline{\xi}+Vt\right)k^2,$$

$$\frac{d\overline{\xi}}{dt}=kq\left(\overline{\xi}+Vt\right), \tag{6.26}$$

where $A_0=A(0)$. We now select the spatial variation of SOD in the form corresponding to an exponentially decreasing profile of the SOD,

$$q=q_0\exp(-\nu x/V). \tag{6.27}$$

In particular, the realization of fibers with exponentially decreasing profiles of the SOD was demonstrated experimentally in [44]. Such profiles are created by variation of the fiber's diameter. Then system (6.14)–(6.18), with the time, wavenumber and the soliton's coordinate redefined as $\theta\equiv\nu t$, $y\equiv k\sqrt{3q_0}/A_0, \eta\equiv\nu\overline{\xi}/V$, is reduced to

$$2\sigma\exp\theta\frac{dy}{d\theta}=-\lambda\exp(3\eta)+y^2\exp(-\eta)+\exp(\eta), \tag{6.28}$$

$$\sigma\exp\theta\frac{d\eta}{d\theta}=y\exp(-\eta), \tag{6.29}$$

where new constants are defined as $\sigma\equiv V\sqrt{3}/\left(A_0\sqrt{q_0}\right), y_0=y(0), \lambda\equiv(8/5)\mu A_0^2V/\nu$. An equilibrium state of Eqs. (6.25)–(6.26) is achieved under conditions

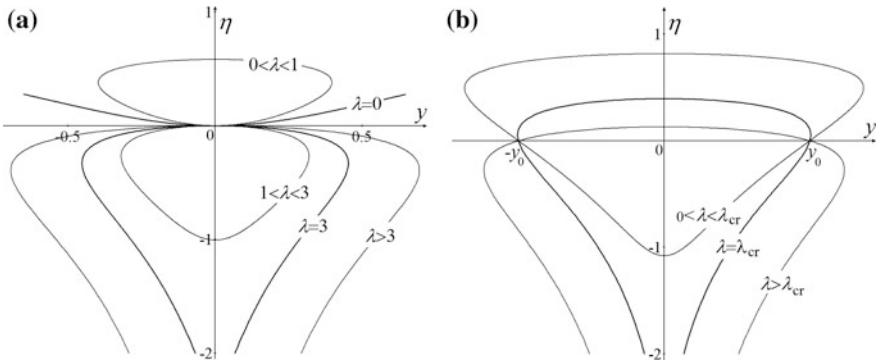

Fig. 6.2 First integral (6.31) in the plane (y, η) of the soliton's rescaled wavenumber and coordinate for $y_0 = 0$ (**a**) and $0 < y_0^2 < 1$ (**b**), and different values of constant λ

$$k_* = 0, \eta_* = -(1/2)\ln\lambda. \tag{6.30}$$

In the equilibrium regime, the wave packet W propagates with the integral moment, N, keeping their initial value, N, and zero wavenumber. Therefore, the field moments for original wave packet, $U = W\exp(-\theta/2)$ decay exponentially, $N_U(\theta) = N\exp(-\theta)$, that $\theta \equiv \nu t$. The first integral of these equations is

$$3y^2\exp(-\eta) + \lambda[\exp(3\eta) - 1] + 3[1 - \exp(\eta)] = 3y_0^2. \tag{6.31}$$

In Fig. 6.2a, first integral (6.31) is drawn in the plane of (y, η) for $y_0 = 0$ and different values of λ. Trajectories in the plot are closed for $0 < \lambda < 3$, and open otherwise. In Fig. 6.2b, first integral (6.31) is drawn in the plane of (y, η) for $0 < y_0^2 < 1$ and different values of λ. Trajectories in the plot are closed for $0 < \lambda < \lambda_{\rm cr} \equiv 3\left(1 - y_0^2\right)$, and open otherwise, cf. Fig. 6.1. The temporal evolution $y(\theta)$ following from Eqs. (6.28)–(6.29) is shown in Fig. 6.3 for initial condition $y_0 = 0$ with different σ and λ.

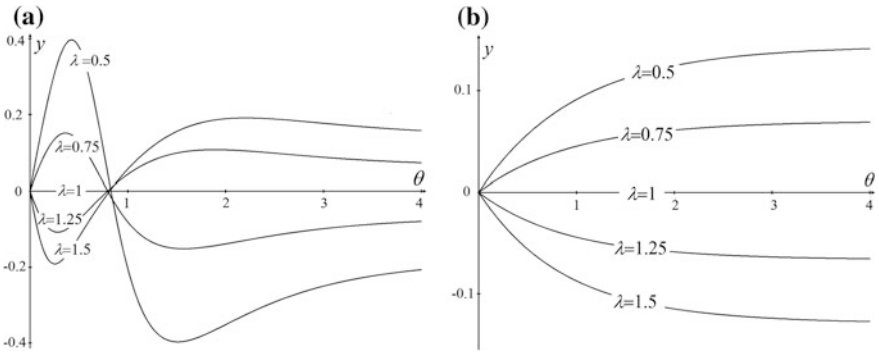

Fig. 6.3 Time evolution $y(\theta)$ obtained from Eqs. (6.28)–(6.29) for initial condition $y_0 = 0$ with different values of σ [**a**: $\sigma = 1/10$, **b**: $\sigma = 1$], and different λ

6.4 Soliton in a Higher-Order Nonlinear Schrödinger Equation with Pseudo-Raman Effect and Inhomogeneous Second-Order Diffraction

Here we consider the dynamics of the HF wave, field $U(\xi,t)\exp(-i\omega t+i\kappa\xi)$, in the framework of inhomogeneous higher-order NLSE with pseudo-Raman, nonlinear-dispersion, TOD and inhomogeneous-SOD terms:

$$2i\frac{\partial U}{\partial t}+\frac{\partial}{\partial\xi}\left[q(\xi)\frac{\partial U}{\partial\xi}\right]+2U|U|^2+2i\chi\frac{\partial\left(U|U|^2\right)}{\partial\xi}+i\gamma\frac{\partial^3U}{\partial\xi^3}+\mu U\frac{\partial\left(|U|^2\right)}{\partial\xi}=0, \tag{6.32}$$

where the following notation is used: μ is, as above, the pseudo-SRS strength, χ is the nonlinear dispersion, and γ is the TOD. Equation (6.1) with zero boundary conditions on infinity, $U|_{\xi\to\pm\infty}\to 0$, gives rise to the following evolution equations for integral moments:

$$\frac{dN}{dt}\equiv\frac{d}{dt}\int_{-\infty}^{+\infty}|U|^2d\xi=0, \tag{6.33}$$

$$2\frac{d}{dt}\int_{-\infty}^{+\infty}K|U|^2d\xi=-\mu\int_{-\infty}^{\infty}\left[\frac{\partial\left(|U|^2\right)}{\partial\xi}\right]^2d\xi-\int_{-\infty}^{\infty}\frac{dq}{d\xi}\left|\frac{\partial U}{\partial\xi}\right|^2d\xi, \tag{6.34}$$

$$N\frac{d\bar{\xi}}{dt}\equiv\frac{d}{dt}\int_{-\infty}^{\infty}\xi|U|^2d\xi=\int_{-\infty}^{+\infty}qK|U|^2d\xi+\frac{3}{2}\chi\int_{-\infty}^{+\infty}|U|^4d\xi-\frac{3}{2}\gamma\int_{-\infty}^{\infty}\left|\frac{\partial U}{\partial\xi}\right|^2d\xi. \tag{6.35}$$

For analytical consideration of the system (6.33)–(6.35), we assume that values of nonlinear dispersion, TOD, and wavenumber are small, $\chi,\gamma,K\sim\varepsilon\ll 1$. In this case, from the imaginary part of (6.32), where terms of order ε^2 are neglected, we derive equation

$$\frac{\partial\left(|U|^2\right)}{\partial t}+\frac{\partial}{\partial\xi}\left(qK|U|^2+\frac{3}{2}\chi|U|^4\right)+\gamma|U|\frac{\partial^3(|U|)}{\partial\xi^3}=0. \tag{6.36}$$

Assuming that wave packets move keeping their shapes, $\partial\left(|U|^2\right)/\partial t\approx -V\partial\left(|U|^2\right)/\partial\xi$, where V is the velocity of the packet, we obtained from Eq. (6.36)

$$\frac{\partial}{\partial\xi}\left(-V|U|^2+qK|U|^2+\frac{3}{2}\chi|U|^4\right)+\gamma|U|\frac{\partial^3(|U|)}{\partial\xi^3}=0. \tag{6.37}$$

Integrating (6.37) for localized wave packets, $|U|_{\xi\to-\infty}\to 0$, and assuming (as above) that the scale of the inhomogeneity of SOD is much larger than the inhomogeneity scale of the wave-packet envelope, $D\gg D_{|U|}$, gives rise to a relation for the wavenumber:

$$K=k(t)-\frac{3\chi}{2q(\bar{\xi})}|U|^2+\frac{3\gamma}{2q(\bar{\xi})|U|^2}\left[\frac{\partial(|U|)}{\partial\xi}\right]^2-\frac{\gamma}{2q(\bar{\xi})|U|^2}\frac{\partial^2\left(|U|^2\right)}{\partial\xi^2}, \tag{6.38}$$

where $k(t)=V/q\left(\bar{\xi}(t)\right)$. Solution of the system of Eqs. (6.34) and (6.35) can be found in the adiabatic approximation, presenting the solution in sech-like form with wavenumber distribution (6.38):

$$U(\xi,t)=A(t)\mathrm{sech}\left[\frac{\xi-\bar{\xi}}{\Delta(t)}\right]\exp\left[i\int K(\xi,t)d\xi-\frac{i}{2}\int A^2(t)dt\right], \tag{6.39}$$

$$K(\xi,t)=k(t)-\frac{3}{2}\frac{\chi A^2(t)}{q(\bar{\xi})}\mathrm{sech}^2\left[\frac{\xi-\bar{\xi}}{\Delta(t)}\right]-\frac{3}{2}\frac{\gamma}{q(\bar{\xi})\Delta^2(t)}\tanh^2\left[\frac{\xi-\bar{\xi}}{\Delta(t)}\right]+\frac{\gamma}{q(\bar{\xi})\Delta^2(t)}, \tag{6.40}$$

where $\Delta(t)\equiv\sqrt{q(\bar{\xi})}/A(t)$ and $A^2(t)\Delta(t)=\mathrm{const}$. Solution (6.39)–(6.40) has two free parameters: an additional wavenumber $k(t)$ and a center-of-mass coordinate $\bar{\xi}(t)$. Substituting Eqs. (6.39)–(6.40) in (6.34)–(6.35) and keeping terms of order ε, we derive a system of equations for k and $\bar{\xi}$:

$$2\frac{dk}{dt}=-\frac{8q_0^2A_0^4\mu}{15q^3(\bar{\xi})}-\frac{q_0A_0^2q'(\bar{\xi})}{3q^2(\bar{\xi})}+\frac{2q_0\gamma A_0^2q'(\bar{\xi})k}{q^3(\bar{\xi})}-\frac{2\chi A_0^2q'(\bar{\xi})k}{q^2(\bar{\xi})}-q'(\bar{\xi})k^2,$$

$$\frac{d\bar{\xi}}{dt}=qk, \tag{6.41}$$

where $q_0=q(0), A_0=A(0)$, and $q'(\bar{\xi})=(dq/d\xi)_{\bar{\xi}}$. System (6.41) gives rise to an obvious equilibrium state (alias a fixed point, FP): $8q_0A_0^2\mu=-5q'(\bar{\xi}_*)q(\bar{\xi}_*), k_*=0$. In particular, for $\mu=\mu_*\equiv-5q'(0)/(8A_0^2)$ the FP corresponds to initial soliton parameters: $\bar{\xi}=0,\ k=0$. For $\mu\neq\mu_*$ soliton's parameters are time-varying. To analyze the evolution around the FP, we assume linearly decreasing SOD, $q'=\mathrm{const}<0$, and rescale the variables by defining $\tau\equiv-tq'A_0/\sqrt{3q_0}, y\equiv k\sqrt{3q_0}/A_0$ and $n=q(\bar{\xi})/q_0$. Then system (6.41) is reduced to

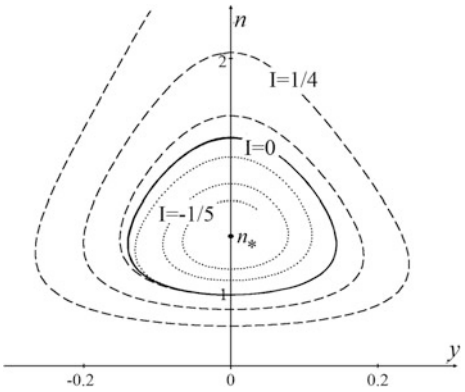

Fig. 6.4 Trajectories (6.42) in the plane (y, n) for $\lambda = 5/4$, initial conditions $y_0 = 0, n_0 \equiv 1$, and different values of $\mathrm{I} = \upsilon - (5/4)\varsigma \equiv \upsilon - \lambda\varsigma$

$$2\frac{dy}{d\tau} = -\frac{\lambda}{n^3} + \frac{1}{n^2} + y^2 - \upsilon\frac{y}{n^3} + \varsigma\frac{y}{n^2}, \quad \frac{dn}{d\tau} = -ny, \tag{6.42}$$

where $\lambda \equiv -8\mu A_0^2/\left(5q^{'}\right) \equiv \mu/\mu_*, \upsilon \equiv 2\sqrt{3}\gamma A_0/\sqrt{q_0^3}, \varsigma \equiv 2\sqrt{3}\chi A_0/\sqrt{q_0^3}$. The FP of Eq. (6.42) in the rescale variables is $y_* = 0, n_* = \lambda$. For $\mathrm{I} \equiv \upsilon - \lambda\varsigma > 0$ the FP is a stable focus, for $\mathrm{I} = 0$ it is a center, and for $\mathrm{I} < 0$ the FP is an unstable focus. Trajectories in the (y, n) plane, obtained from Eq. (6.42) with initial conditions $y_0 = 0, n_0 \equiv 1$ for $\lambda = 5/4$, and different values of $\mathrm{I} = \upsilon - (5/4)\varsigma \equiv \upsilon - \lambda\varsigma$, are shown in Fig. 6.4.

For $\mu = \mu_* \equiv 5q^{'}/\left(8A_0^2\right)$, corresponding to $\lambda = 1$, the FP's coordinates coincide with the initial soliton parameters, $n_0 \equiv 1, y_0 = 0$. In this case, the soliton's parameters remain constant in time.

6.5 Vector Solitons in Coupled Nonlinear Equations with the Pseudo-Raman Effect and Inhomogeneous Dispersion

We consider dynamics of the two-component (vector) HF wave field $\vec{E}(\xi, t) = U_1(\xi, t)\exp(i\omega t - i\kappa\xi)\vec{e}_1 + U_2(\xi, t)\exp(i\omega t - i\kappa\xi)\vec{e}_2$, where $\vec{e}_{1,2}$ are unit vectors of two orthogonal polarizations, and $U_{1,2}$ are the corresponding amplitudes. The consideration is carried out in the framework of two coupled NLSEs including pseudo-SRS, cross-pseudo-SRS, XPM and inhomogeneous SOD:

$$2i\left(\frac{\partial U_{1,2}}{\partial t}\mp\delta\frac{\partial U_{1,2}}{\partial\xi}\right)+\frac{\partial}{\partial\xi}\left[q(\xi)\frac{\partial U_{1,2}}{\partial\xi}\right]$$
$$+2U_{1,2}\left(|U_{1,2}|^2+|U_{2,1}|^2\right)+\mu U_{1,2}\frac{\partial\left(|U_{1,2}|^2+|U_{2,1}|^2\right)}{\partial\xi}=0, \tag{6.43}$$

where δ is the group-velocity mismatch between the components, and μ is, once again, the pseudo-SRS strength. The substitution of $U_{1,2}=u_{1,2}\exp\left[\pm i\delta\int d\xi/q(\xi)\right]$ transforms Eq. (6.43) into

$$2i\frac{\partial u_{1,2}}{\partial t}+\frac{\partial}{\partial\xi}\left[q(\xi)\frac{\partial u_{1,2}}{\partial\xi}\right]+\frac{\delta^2}{q(\xi)}u_{1,2}+2u_{1,2}\left(|u_{1,2}|^2+|u_{2,1}|^2\right)+\mu u_{1,2}\frac{\partial\left(|u_{1,2}|^2+|u_{2,1}|^2\right)}{\partial\xi}=0, \tag{6.44}$$

with an effective potential $\delta^2/q(\xi)$ (this definition implies that $q(\xi)$ does not vanish; it may be interesting too to consider a setting with a zero-dispersion point, at which $q(\xi)=0$, but in that case it necessary to take into regard the third-order-dispersion term, which is not included here).

6.5.1 Analytical Results

Equation (6.44) with zero boundary conditions at infinity, $u_{1,2}|_{\xi\to\pm\infty}\to 0$, gives rise to the following exact integral relations for a localized wave packet:

$$\frac{dN_{1,2}}{dt}\equiv\frac{d}{dt}\int_{-\infty}^{+\infty}|u_{1,2}|^2d\xi=0, \tag{6.45}$$

$$2\frac{d}{dt}\int_{-\infty}^{+\infty}k_{1,2}|u_{1,2}|^2d\xi=-\mu\int_{-\infty}^{\infty}\frac{\partial\left(|u_{1,2}|^2\right)}{\partial\xi}\frac{\partial\left(|u_{1,2}|^2+|u_{2,1}|^2\right)}{\partial\xi}d\xi-\int_{-\infty}^{\infty}\frac{dq}{d\xi}\left(\left|\frac{\partial u_{1,2}}{\partial\xi}\right|^2+\frac{\delta^2}{q^2}|u_{1,2}|^2\right)d\xi$$
$$+2\int_{-\infty}^{+\infty}|u_{1,2}|^2\frac{\partial\left(|u_{2,1}|^2\right)}{\partial\xi}d\xi, \tag{6.46}$$

$$N_{1,2}\frac{d\bar{\xi}_{1,2}}{dt}\equiv\frac{d}{dt}\int_{-\infty}^{\infty}\xi|u_{1,2}|^2d\xi=\int_{-\infty}^{+\infty}qk_{1,2}|u_{1.2}|^2d\xi, \tag{6.47}$$

where $u_{1,2}=|u_{1,2}|\exp\left(i\varphi_{1,2}\right)$, and $k_{1,2}=\partial\varphi_{1,2}/\partial\xi$ are wavenumbers of wave packets $u_{1,2}$.

To analyze of the wave-packet dynamics, we assume, as above, that the scale of the spatial inhomogeneity of SOD is much larger than the packet's width, $D_q \gg \Delta$. A solution to system (6.3)–(6.5) is then looked for in the form of a sech ansatz, with two components proportional to each other:

$$u_1(\xi,t)=A(t)\mathrm{sech}\left[\frac{\xi-\overline{\xi}(t)}{\Delta(t)}\right]\exp\left[ik(t)\xi-i\int\Omega(t)dt\right],\quad u_2(\xi,t)=\sigma u_1(\xi,t), \tag{6.48}$$

where σ is a free real parameter, $\overline{\xi}(t)=\overline{\xi}_{1,2}(t)$ is the coordinate of the soliton's center $2\Omega(t)=(1+\sigma^2)A^2(t)+\delta^2/q\left(\overline{\xi}(t)\right)$, $\Delta(t)=(1/A(t))\sqrt{q\left(\overline{\xi}(t)\right)/(1+\sigma^2)}$ $k(t)\equiv k_{1,2}(t)$, and it is set $A^2(t)\Delta(t)=\mathrm{const}$, which is the usual relation between the amplitude and width of sech-shaped solitons. Substituting ansatz (6.48) in Eqs. (6.46) and (6.47), and taking into account the above condition $\Delta \ll D_q$, leads to the following evolution equations:

$$2\frac{dk}{dt}=-\mu\frac{8}{15}\frac{(1+\sigma^2)^2q_0^2A_0^4}{q^3\left(\overline{\xi}\right)}-\frac{(1+\sigma^2)q_0A_0^2q'\left(\overline{\xi}\right)}{3q^2\left(\overline{\xi}\right)}-\frac{\delta^2q'\left(\overline{\xi}\right)}{q^2\left(\overline{\xi}\right)}-q'\left(\overline{\xi}\right)k^2,$$

$$\frac{d\overline{\xi}}{dt}=kq\left(\overline{\xi}\right), \tag{6.49}$$

where initial values are $q_0\equiv q\left(\overline{\xi}(t=0)\right)$, $A_0\equiv A(t=0)$, which obey the above-mention relation, $A^2(t)q\left(\overline{\xi}(t)\right)=A^2(t=0)q\left(\overline{\xi}(t=0)\right)\equiv A_0^2q_0$, and $q'\left(\overline{\xi}\right)\equiv dq/d\xi|_{\xi=\overline{\xi}}$ is the derivative (*slope*) of the SOD coefficient at the soliton's center. Equation (6.49) give rise to an obvious equilibrium state (alias a fixed point, FP):

$$8\mu\left(1+\lambda^2\right)^2q_0^2A_0^4=-5q'\left(\overline{\xi}_*\right)q\left(\overline{\xi}_*\right)\left[\left(1+\lambda^2\right)q_0A_0^2+3\delta^2\right],\ k_*=0, \tag{6.50}$$

where $\overline{\xi}_*$ is the equilibrium position of the soliton. In the particular case of $\lambda=\delta=0$, relation (6.50) reduces to its counterpart for the single NLSE derived in [38]. For $\mu=\mu_*\equiv-(5/8)q'\left(\overline{\xi}_0\right)\left[(1+\sigma^2)q_0A_0^2+3\delta^2\right]/\left[(1+\sigma^2)^2q_0A_0^4\right]$ the equilibrium position of the soliton coincides with its initial position, $\overline{\xi}_*=\overline{\xi}_0\equiv\overline{\xi}(t=0)$.

To analyze the evolution near the FP, we assume a constant value of the SOD slope around the FP, $q'=\mathrm{const}$, and rescale the variables by defining $\tau\equiv-tq'\sqrt{q_0A_0^2(1+\sigma^2)+3\delta^2}/\left(\sqrt{3}q_0\right)$, $y(\tau)\equiv k(\tau)-tq'\sqrt{3}q_0/\sqrt{q_0A_0^2(1+\sigma^2)+3\delta^2}n(\tau)\equiv q\left(\overline{\xi}(\tau)\right)/q_0$, thus deriving a simple mechanical system from Eq. (6.49), coinciding with Eq. (6.11).

Here we address steady-state solutions of Eq. (6.44) for a linear profile of the inhomogeneous SOD, viz., $q(\xi)=q_0+q'\xi$, in the form of $U_2(\xi,t)=\sigma U_1(\xi,t)\equiv\sigma\psi(\xi)\exp(i\Omega t)$:

$$-2\Omega\psi+\frac{\delta^2}{q_0+q'\xi}\psi+\left(q_0+q'\xi\right)\frac{d^2\psi}{d\xi^2}+q'\frac{d\psi}{d\xi}+2\left(1+\sigma^2\right)\psi^3+\mu\left(1+\sigma^2\right)\psi\frac{d\left(\psi^2\right)}{d\xi}=0. \tag{6.51}$$

Similar to what was adopted above, we again assume that the wave-packet's width is much smaller than the scale of the SOD's spatial inhomogeneity, $\Delta\ll 1/\left|q'\right|$. Introducing the corresponding small parameter, $\varepsilon\sim\Delta\cdot q'\sim\mu\ll q_0$, a solution to Eq. (6.51) can be looked for as $\psi=\Phi+\phi$, where ϕ is a correction $\sim\varepsilon$. Separating terms of orders ε^0 and ε^1, we obtain

$$q_0\frac{d^2\Phi}{d\xi^2}+2\Phi^3\left(1+\sigma^2\right)-\left(2\Omega-\frac{\delta^2}{q_0}\right)\Phi=0, \tag{6.52}$$

$$q_0\frac{d^2\phi}{d\xi^2}+\left[6\left(1+\sigma^2\right)\Phi^2-2\Omega+\frac{\delta^2}{q_0}\right]\phi=q'\frac{\delta^2}{q_0^2}\Phi\xi-q'\frac{d^2\Phi}{d\xi^2}\xi-q'\frac{d\Phi}{d\xi}-\frac{2}{3}\mu\left(1+\sigma^2\right)\frac{d\left(\Phi^3\right)}{d\xi}. \tag{6.53}$$

Equation (6.52) has the standard sech-soliton solution, $\Phi=A\,\mathrm{sech}(\xi/\Delta)$, where $\Delta=\sqrt{q_0/(1+\sigma^2)}/A$, and $2\Omega=(1+\sigma^2)A^2+\delta^2/q_0$. Then, in terms of rescaled variables, $\eta\equiv\xi/\Delta$ and $\phi\equiv q'\Psi/\sqrt{q_0\left(1+\lambda^2\right)}$, Eq. (6.53) takes the form of

$$\begin{aligned}&\frac{d^2\Psi}{d\eta^2}+\left(\frac{6}{\cosh^2\eta}-1\right)\Psi\\&=\left[\frac{\delta^2}{q_0(1+\sigma^2)A_0^2}-1\right]\frac{\eta}{\cosh\eta}+\frac{2\eta}{\cosh^3\eta}+\frac{\sinh\eta}{\cosh^2\eta}+\frac{2\mu(1+\sigma^2)A_0^2}{q'}\frac{\sinh\eta}{\cosh^4\eta}.\end{aligned} \tag{6.54}$$

An essential result is that, at

$$\mu=\mu_*\equiv-(5/8)q'(1+3\mathrm{H})/\left[\left(1+\sigma^2\right)A_0^2\right], \tag{6.55}$$

where $\mathrm{H}\equiv\delta^2/\left[q_0(1+\sigma^2)A_0^2\right]$, Eq. (6.54) has an *exact* localized solution for the correction to the standard sech soliton,

$$\Psi(\eta)=(1/4)(\mathrm{sech}\eta)\left[2\mathrm{H}\eta+(1-\mathrm{H})\eta^2\tanh\eta-(1+3\mathrm{H})(\tanh\eta)\ln(\cosh\eta)\right]. \tag{6.56}$$

In the particular case of $H=0$, which corresponds to $\delta=0$, i.e., in the absence of the group-velocity mismatch between the polarization components, solution (6.56) carries over into one obtained above in Sect. 6.2, see Eq. (6.17).

6.5.2 Numerical Results

To check the above analytical results, we here aim to report findings produced bysimulations of the evolution of initial wave packet $u_{1,2}(\xi,0)=\left(1/\sqrt{2}\right)\mathrm{sech}\xi$ in the framework of Eq. (6.44) with a typical linear profile of the inhomogeneous SOD, $q=1-\xi/20, \delta=1, \sigma=1$ and different values of strength μ of the pseudo-SMS effect. The respective point (6.50) of the equilibrium between the pseudo-SRS and inhomogeneous SOD is $\mu_*=1/8$. In the simulations performed with $\mu=1/8$, at times $t>10$ the pulse evolves into a stationary localized profile with zero wavenumber. Figure 6.5 shows the deviation of the absolute value of the numerically found stationary profile from the sech-soliton input, i.e., $\phi_{\mathrm{num}}(\xi)=|u_{1,2}(\xi)|-\left(1/\sqrt{2}\right)\mathrm{sech}\xi$ (the solid curve in the figure). The deviation is very close to the respective analytically predicted correction, given by Eq. (6.56):

$$\phi=-\left(\sqrt{2}/80\right)(\mathrm{sech}\xi)[\xi-2\tanh\xi\,\ln(\cosh\xi)], \tag{6.57}$$

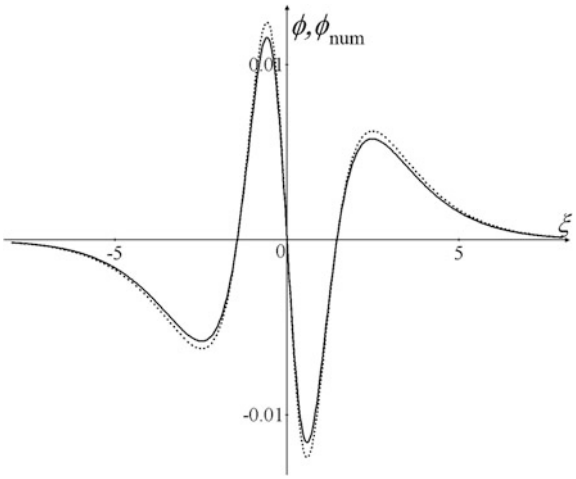

Fig. 6.5 Numerical results: deviation of the absolute value of the numerically found stationary pulse from the standard soliton shape, $\phi_{\mathrm{num}}(\xi)=|u_{1,2}(\xi)|-\left(1/\sqrt{2}\right)\mathrm{sech}\xi$ (the solid curve). The analytical correction ϕ to the absolute value of the standard soliton solution, given by Eq. (6.57), is shown by the dashed curve

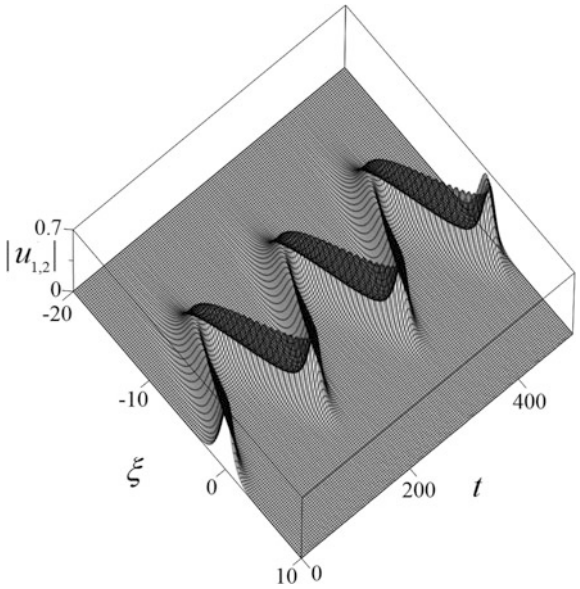

Fig. 6.6 Results of the simulations of the evolution of the sech-shaped pulse for $\mu = (4/3)\mu_* \equiv 1/6$

as shown by the dashed curve in Fig. 6.5. Change of the pseudo-SMS strength μ leads to variation of soliton's wavenumber and amplitude. In particular, Fig. 6.6 shows the simulated spatiotemporal evolution of $|u_{1,2}(\xi, t)|$ for $\mu = (4/3)\mu_* \equiv 1/6$. In this case, the soliton performs oscillations without any visible radiation loss, i.e., the soliton is dynamically stable in the case, in the oscillatory state.

The above considerations were focused on two-component solitons with similar shapes of the components. It is an issue of straightforward interest too to consider the evolution of inputs with opposite parities of the components. For this purpose, we carried out the simulations initiated by the input with an even profile in one component, and an odd one in the other:

$$u_1(\xi, 0) = \mathrm{sech}\xi, u_2(\xi, 0) = A[\mathrm{sech}(\xi + 1) - \mathrm{sech}(\xi - 1)], \tag{6.58}$$

in the framework of Eq. (6.44) with $q = 1 - x/20, \delta = 0$, and different values of A and μ. Figures 6.7, 6.8, and 6.9 display the resulting spatiotemporal evolution of $|u_1(\xi, t)|$ (a) and $|u_2(\xi, t)|$ (b). For the relative amplitude of the odd component $A = 0.8$ (with $\mu = 1/10$), initial pulse (6.58) transforms into an *essentially novel* dynamical mode, in the form of a breather which keeps the opposite parities in its components (Fig. 6.7). Further, for $A = 1$ (with $\mu = 1/25$) initial pulse (6.58) splits into two separating vector solitons of the usual type, with identical parities in the two components (Fig. 6.8), which is possible as the odd component in Eq. (6.58), $u_2(\xi, 0)$, is built as a set of two pulses with opposite signs. Lastly, for $A = 0.5$ (with

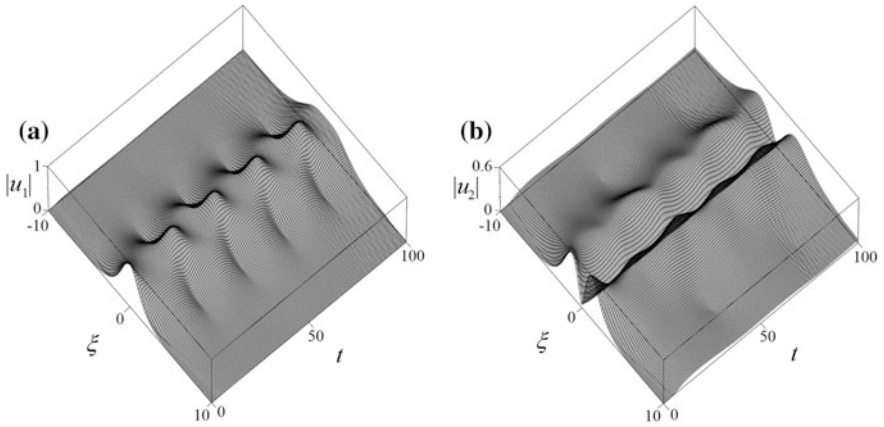

Fig. 6.7 The result of simulations of the evolution of the initial pulse (6.58) with opposite parities of the components, for $A = 0.8$ and $\mu = 1/10$: formation of a breather with coupled even and odd components

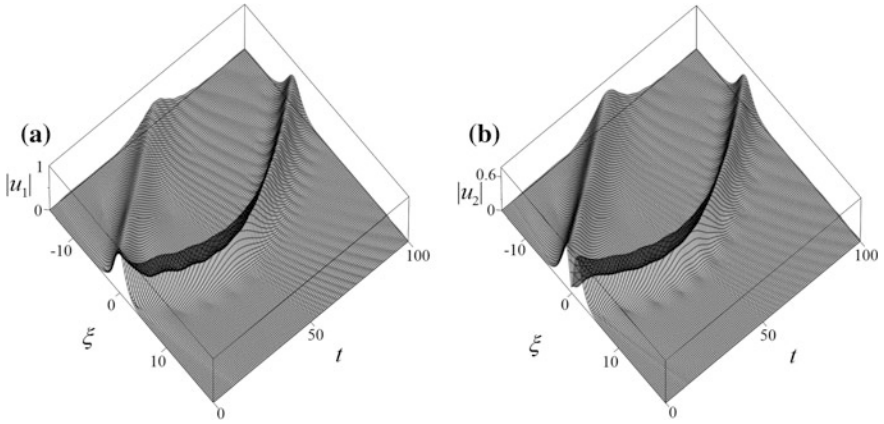

Fig. 6.8 The result of simulations of the evolution of the initial pulse (6.58) for $A = 1$ and $\mu = 1/25$: splitting into two vector solitons of the usual type

$\mu = 1/30$) the weaker component u_2 tends to spread out into a small-amplitude pedestal, into which a dark soliton is embedded (Fig. 6.9b), while the even component u_1 shows no essential evolution (Fig. 6.9a). In the latter case, the u_2 component keeps the spatially odd structure, as dark solitons are odd kink-like solutions.

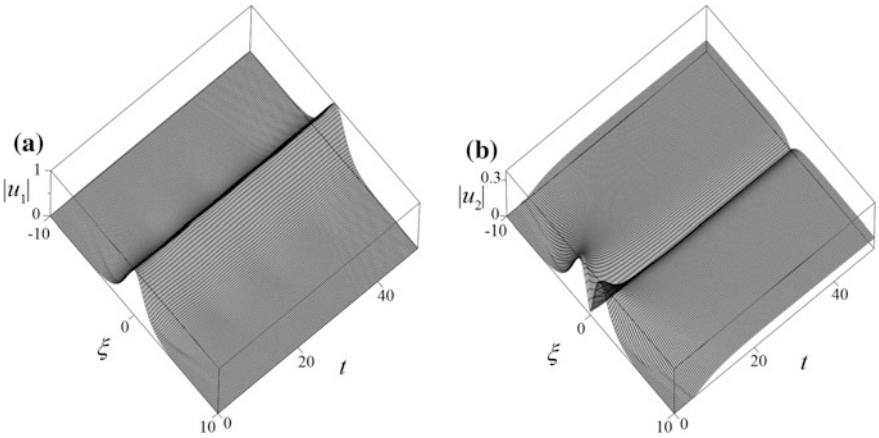

Fig. 6.9 The result of simulations of the evolution of the initial pulse (6.58) for $A = 0.5$ and $\mu = 1/30$: the transformation of the weak odd component into a small-amplitude dark soliton

6.6 Solitons in a Forced Nonlinear Schrödinger Equation with the Pseudo-Raman Effect

In this section, we consider the unidirectional copropagating of a slowly varying envelope, $U(x,t)$, of the complex HF wave field, $U(x,t)\exp(ik_0x - i\omega_0 t)$, and its real LF counterpart, $n(x,t)$ (as said above, it may be realized as a local perturbation of the refractive index, in terms of the optical or quasi-optical propagation). If the HF and LF fields represent the SW (surface waves) and IW (internal waves), respectively, in the ocean, the corresponding Zakharov-type system is composed of the Schrödinger equation for the SW and Boussinesq (Bq) equation for the IW, coupled by the quadratic terms [45–48]. Although the underlying geometry of the fluid motion is two-dimensional, the derivation of the coupled system simplifies the model to the one-dimensional form, as the crucially important geometric elements which guide the propagating waves, viz., the free surface and interface between the layers with different densities of water, are one-dimensional. Under the commonly adopted assumption of the unidirectional wave propagation, the Bq equation may be reduced to one of the Korteweg–de Vries type. Taking into regard LF viscosity δ and the linear gain with real coefficient β applied to the SW, which, as said above, represents the wind forcing in the ocean [49], the system of equations takes the form of:

$$2i\left(\frac{\partial U}{\partial t} + V\frac{\partial U}{\partial x}\right) - \frac{\partial^2 U}{\partial x^2} - \beta\frac{\partial U}{\partial x} - nU = 0, \tag{6.59}$$

$$\frac{\partial n}{\partial t} + V_L \frac{\partial n}{\partial x} - \delta \frac{\partial^2 n}{\partial x^2} = -\frac{\partial \left(|U|^2 \right)}{\partial x}, \tag{6.60}$$

where V and V_L are the HF and LF group velocities.

The interplay of the wind, SW and IW is strong enough if the group velocities of the SW and IW at some (widely different, see below) wavelengths, $\Lambda_{\rm SW}$ and $\Lambda_{\rm IW}$, are in resonance, and, additionally, the wind's friction velocity, W, is in resonance with the SW group velocity [45, 49]. Taking a characteristic value, $W \sim 10$ cm/s [50], the classical dispersion relation for the SW on deep water, $\omega_{\rm SW} = \sqrt{gk}$, and the characteristic value for the Brunt-Väisälä (buoyancy) frequency, $\omega_{\rm BV} \sim 0.01$ Hz, which gives rise to the IW at the interface between the top mixed layer and the underlying undisturbed one in the ocean (at the depth of a few hundred meters) [51], one can conclude that the corresponding characteristic HF is $\omega_{\rm SW} \sim 50$ Hz, which exceeds the above-mentioned LF, $\omega_{\rm BV}$ by three or four orders of magnitude, thus completely justifying the HF-LF frequency distinction. The difference in the respective wavelength is dramatic too, the estimate yielding $\Lambda_{\rm SW} \sim 2$ cm and $\Lambda_{\rm IW} \sim 10$ m.

In the third-order approximation of the theory (see Sect. 6.2) system (6.59)–(6.60) leads to the following evolution equation for the HF envelope amplitude:

$$2i \frac{\partial U}{\partial t} = \frac{\partial^2 U}{\partial \xi^2} + \beta \frac{\partial U}{\partial \xi} + 2\alpha U |U|^2 - \mu U \frac{\partial \left(|U|^2 \right)}{\partial \xi}, \tag{6.61}$$

where $\xi \equiv x - Vt, \alpha \equiv (1/2)(V - V_L)^{-1}, \mu \equiv \delta (V_L - V)^{-2}$. Below, we fix $\alpha = 1$ by means of obvious scaling, as it was done above in a different context.

The gain term in Eq. (6.61) may be formally absorbed by a transition into a reference frame moving with imaginary velocity, i.e., replacement of real coordinate ξ by $\Xi \equiv \xi - i(\beta/2)t$, which makes it possible to obtain exact soliton solutions to Eq. (6.62) that explicitly feature growth effects induced by the gain [49]. However, we prefer to consider Eq. (6.61) in terms of the real coordinate and time. Then, it is natural to analyze the dispersion relation for small-amplitude excitations, governed by the linearized versions of Eq. (6.61), by substituting $U \sim \exp(i\kappa\xi - i\omega t)$, which produces a complex frequency as a function of real wavenumber κ:

$$\omega = -\kappa^2/2 + (i/2)\beta\kappa.$$

The same branch of the HF dispersion relation is valid for system (6.59)–(6.60), as the nonlinear HF-LF coupling does not affect the dispersion relation. The real part of the frequency gives rise to the group velocity, $V_{\rm gr} \equiv d\omega/d\kappa = -\kappa$, hence the excitation traveling at this velocity grows with the distance, $-\xi$, as

$$U \sim \exp(\mathrm{Im}\omega \cdot t) \equiv \exp\left(\mathrm{Im}\omega \cdot \xi / V_{\mathrm{gr}}\right) = \exp(-\beta\xi/2) \tag{6.62}$$

(note that it does not depend on the wavenumber, κ), which represents a typical manifestation of the *convective instability* [52]. This type of the instability implies that (in contrast with the *absolute instability*, which drives the growth of quiescent perturbations), the perturbations grow as they travel away, hence they usually do not destroy the underlying patterns. Namely, if a soliton of size L, maintained by the balance between the linear gain and pseudo-SRS term, does not move on the average (see below), it follows from Eq. (6.62) that the soliton is not hurt by the convective instability, provided that it is narrow enough, $\mathrm{L} \ll \beta^{-1}$.

Equation (6.61) with zero boundary conditions at infinity, $U|_{\xi \to \pm\infty} \to 0$, gives rise to the following integral relations for field moments:

$$\frac{dN}{dt} \equiv \frac{d}{dt} \int_{-\infty}^{+\infty} |U|^2 d\xi = \beta \int_{-\infty}^{+\infty} k|U|^2 d\xi \equiv -\beta P, \tag{6.63}$$

$$\frac{dP}{dt} = -\beta \int_{-\infty}^{+\infty} \left|\frac{\partial U}{\partial \xi}\right|^2 d\xi + \frac{\mu}{2} \int_{-\infty}^{+\infty} \left[\frac{\partial\left(|U|^2\right)}{\partial \xi}\right]^2 d\xi, \tag{6.64}$$

$$\frac{d}{dt} \int_{-\infty}^{+\infty} \xi |U|^2 d\xi = P + \beta \int_{-\infty}^{+\infty} k\xi |U|^2 d\xi, \tag{6.65}$$

The moments introduced in Eqs. (6.63), (6.64), and (6.65) determine the norm, N, momentum, P, and center-of-mass coordinate, $\overline{\xi}$, of the wave packet.

The system of exact evolution equations for the moments may be used, as done above in different contexts, for the derivation of approximate evolution equations for parameters of a soliton, see Refs. [53–56] and references therein. To this end, we adopt the usual ansatz for the moving soliton, with amplitude $A(t)$, wavenumber $k(t)$, and coordinate $\overline{\xi}$ defined above:

$$U(\xi, t) = A(t)\mathrm{sech}\left[A(t)\left(\xi - \overline{\xi}\right)\right] \exp\left[ik(t)\xi - (i/2)\int A^2(t)dt\right]. \tag{6.66}$$

The substitution of the ansatz into Eqs. (6.63)–(6.65) leads to the following evolution equations:

$$\frac{dk}{dt} = \frac{\beta}{3}A^2 - \frac{4}{15}\mu A^4, \frac{dA}{dt} = \beta A k, \frac{d\overline{\xi}}{dt} = -k, \tag{6.67}$$

which give rise to an obvious equilibrium state (alias fixed point, FP):

$$\mu_* \equiv 5\beta/\left(4A_0^2\right), k_* = 0, \tag{6.68}$$

where A_0 is an arbitrary amplitude if the stationary soliton. To analyze the evolution around the FP, we rescale the variables by defining $\tau \equiv t\beta A_0/\sqrt{6}, a \equiv A/A_0, y \equiv k\sqrt{6}/A_0$, thus deriving a simple mechanical system from Eq. (6.67):

$$\frac{dy}{d\tau} = 2a^2\left(1 - \lambda a^2\right), \frac{da}{d\tau} = ay, \tag{6.69}$$

where $\lambda \equiv \mu/\mu_*$. Obviously, Eq. (6.69) conserves the corresponding Hamiltonian,

$$y^2 + \lambda\left(a^4 - 1\right) - 2\left(a^2 - 1\right) = y_0^2, \tag{6.70}$$

where y_0 is the value of y at $a = 1$. Dynamical invariant (6.70) is drawn in the plane of (y, a) in Fig. 6.10a, for $y_0 = 0$ and different values of λ. Evidently, at $\lambda < 1$ (i.e., if the pseudo-SRS effect is relatively weak), the soliton's amplitude periodically oscillates between maximum and minimum values $a_{\max} \equiv A_{\max}/A_0 = \sqrt{(2-\lambda)/\lambda}$ and $a_{\min} = 1$. These values swap if the pseudo-SRS effect is stronger, viz., $1 < \lambda < 2$ (the amplitude remains constant at $\lambda = 1$). As it follows from Eq. (6.70), oscillations of the soliton's amplitude translate into oscillations of its velocity, which are symmetric with respect to the positive and negative values.

Lastly, if the pseudo-SRS term is too large, with $\lambda \geq 2$, it destroys the soliton, as the evolution leads to the decay of the amplitude to $a = 0$, while the rescaled wavenumber takes the limit value $y_\infty \equiv \sqrt{\lambda - 2}$.

Further, at $y_0^2 > 0$ straightforward analysis of Eq. (6.70) demonstrates that the loop trajectories, which are seen in Fig. 6.10a for $y_0^2 = 0$, stretch in both positive and negative vertical directions (along the axis of a). In the same case, the critical value

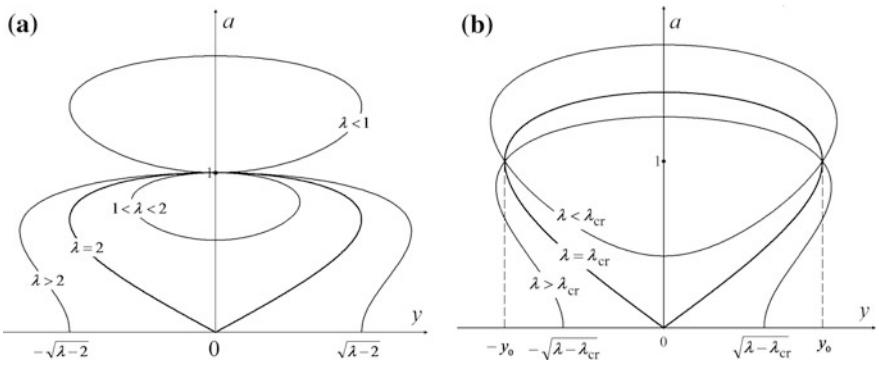

Fig. 6.10 Plots of dynamical invariant (6.70) in plane (y, a) of the soliton's rescaled wavenumber and amplitude for $y_0 = 0$ (**a**) and $0 < y_0^2 < 2$ (**b**), and different values of constant λ

of the pseudo-SRS coefficient, which leads to the destruction of the soliton, decreases to $\lambda_{\rm cr} = 2 - y_0^2$; thus, the solitons do not exist at all at $y_0^2 > 2$. Dynamical invariant (6.70) is schematically drawn in the plane of (y, a) in Fig. 6.10b, for $0 < y_0^2 < 2$ and different values of λ.

6.7 Conclusion

In this article we have produced a review of results obtained in modelsbased on the extended NLSEs (nonlinear Schrödinger equations) which contain the spatial-domain counterpart of the SRS (stimulated Raman scattering) term, viz., the pseudo-SRS one). The NLSEs are derived from the systems of the Zakharov's type for electromagnetic or Langmuir waves in plasmas and similar media, in which the LF field is subject to the diffusive damping. We have studied the soliton dynamics is the framework of the extended NLSEs, which may also include the smooth spatial variation of the SOD (second-order dispersion) coefficient. The analytical predictions were produced by integral relations for the field moments, and numerical results were generated by systematic simulations of the pulse evolution in the framework of the extended NLSEs. Stable stationary solitons are maintained, in particular, by the balance between the self-wavenumber downshift, driven by the pseudo-SRS, and the upshift induced by the linearly decreasing SOD. The analytical solutions are found to be in close agreement with their numerical counterparts.

Acknowledgements The work of B.A.M. is supported, in part, by grant No. 2015616 from the joint program in physics between National Science Foundation (US) and Binational (US-Israel) Science Foundation, and by grant No. 1287/17 from the Israel Science Foundation.

References

1. Infeld, E., Rowlands, G.: Nonlinear Waves, Solitons, and Chaos. Cambridge University Press, Cambridge (2000)
2. Agrawal, G.P.: Nonlinear Fiber Optic. Academic Press, San Diego (2001)
3. Yang, J.: Solitons in Field Theory and Nonlinear Analysis. Springer, New York (2001)
4. Kivshar, Y.S., Agrawal, G.P.: Optical Solitons: From Fibers to Photonic Crystals. Academic, San Diego (2003)
5. Dickey, L.A.: Soliton Equation and Hamiltonian Systems. World Scientific, New York (2005)
6. Malomed, B.A.: Soliton Management in Periodic Systems. Springer, New York (2006)
7. Dauxois, T., Peyrard, M.: Physics of Solitons. Cambridge University Press, Cambridge (2006)
8. Sich, M., Krizhanovskii, D.N., Skolnick, M.S., Gorbach, A.V., Hartley, R., Skryabin, D.V., Cerda-Méndez, E.A., Biermann, K., Hey, R., Santos, P.V.: Observation of bright solitons in a semiconductor microcavity. Santos Nature Phot. **6**, 50–55 (2012)
9. Kauranen, M., Zayats, A.V.: Nonlinear plasmonics. Nature Phot. **6**, 737–748 (2012)

10. Cerda-Ménde, E.A., Sarkar, D., Krizhanovskii, D.N., Gavrilov, S.S., Biermann, K., Skolnick, M.S., Santos, P.V.: Polaritonic two-dimensional nonlinear crystals. Phys. Rev. Lett. **111**, 146401 (2013)
11. Zakharov, V.E., Shabat, A.B.: Exact theory of two-dimensional self-focusing and one-dimensional self-modulation of waves in nonlinear media. Sov. Phys. JETP **34**, 62–69 (1972)
12. Hasegawa, A., Tappert, F.: Transmission of stationary nonlinear optical physics in dispersive dielectric fibers I: anomalous dispersion Appl. Phys. Lett. **23**, 142–144 (1973)
13. Tajima, K.: Compensation of soliton broadening in nonlinear optical fibers with loss. Opt. Lett. **12**, 54–56 (1987)
14. Manakov, S.V.: On the theory of two-dimensional stationary self-focusing of electromagnetic waves. Sov. Phys. JETP **38**, 248–253 (1974)
15. Fordy, A.P., Kullish, P.P.: Commun. Math. Phys. **89**, 427–443 (1983)
16. Menyuk, C.R., Josa, B.: Nonlinear Schrödinger equations and simple Lie algebras **5**, 392–402 (1988)
17. Lazarides, N., Tsironis, G.P.: Coupled nonlinear Schrödinger equations for electromagnetic wave propagation in nonlinear left-handed materials. Phys. Rev. E **71**, 036614 (2005)
18. Yang, J.: Interactions of vector solitons. Phys. Rev. E **64**, 026607 (2001)
19. Ablowitz, M.J., Prinari, B., Trubatch, A.D.: Soliton interactions in the vector NLS equation. Invers. Probl. **20**, 1217–1237 (2004)
20. Vahala, G., Yepes, L.V.: Inelastic vector soliton collisions: a quantum lattice gas representation. J. Phil. Trans. Roy. Soc. L A **362**, 1677–1690 (2004)
21. Oliviera, J.R., Moura, M.A.: Analytical solution for the modified nonlinear Schrödinger equation describing optical shock formation. Phys. Rev. E **57**, 4751–4755 (1998)
22. Mitschke, F.M., Mollenauer, L.F.: Discovery of the soliton self-frequency shift. Opt. Lett. **11**, 659–661 (1986)
23. Gordon, J.P.: Theory of the soliton self-frequency shift. Opt. Lett. **11**, 662–664 (1986)
24. Kodama, Y.: Optical solitons in a monomode fiber. J. Stat. Phys. **39**, 597–614 (1985)
25. Malomed, B.A., Tasgal, R.S.: Matching intrapulse self-frequency shift to sliding-frequency filters for transmission of narrow solitons. J. Opt. Soc. Am. B **15**, 162–170 (1998)
26. Biancalama, F., Skrybin, D.V., Yulin, A.V.: Theory of the soliton self-frequency shift compensation by the resonant radiation in photonic crystal fibers. Phys. Rev. E **70**, 011615 (2004)
27. Essiambre, R.-J., Agraval, G.P.: Timing jitter of ultra short solitons in high-speed communication systems. I. General formulation and application to dispersion-decreasing fibers. J. Opt. Soc. Am. B **14**, 314–322 (1997)
28. Essiambre, R.-J., Agrawal, G.P.: Timing jitter of ultra short solitons in high-speed communication systems. II. Control of jitter by periodic optical phase conjugation. J. Opt. Soc. Am. B **14**, 323–330 (1997)
29. Andrianov, A., Muraviev, S., Kim, A., Sysoliatin, A.: DDF-based all-fiber optical source of femtosecond pulses smoothly tuned in the telecommunication range. Laser Phys. **17**, 1296–1302 (2007)
30. Chernikov, S., Dianov, E., Richardson, D., Payne, D.: Soliton pulse compression in dispersion-decreasing fiber. Opt. Lett. **18**, 476–478 (1993)
31. Kim, J.: A coupled higher-order nonlinear Schrodinger equation including higher-order bright and dark solitons. ETRI J. **23**, 9–15 (2001)
32. Lu, F., Lin, W.H., Knox, W.H., Agrawal, G.P.: Vector soliton fission. Phys. Rev. Lett. **93**, 183901 (2004)
33. Gromov, E.M., Piskunova, L.V., Tyutin, V.V., Vorontzov, D.E.: Short vector solitons. Phys. Lett. A **287**, 233–239 (2001)
34. Wen, S.C., et al.: Theoretical models for ultrashort electromagnetic pulse propagation in nonlinear metamaterials. Phys. Rev. A **75**, 033815 (2007)
35. Aseeva, N.V., Gromov, E.M., Tyutin, V.V.: Phase interaction of short vector solitons. Phys. Lett. A **376**, 718–722 (2012)

36. Gromov, E.M., Malomed, B.A.: Soliton dynamics in an extended nonlinear Schrödinger equation with a spatial counterpart of the stimulated Raman scattering. J. Plasma Phys. **79**, 1057–1062 (2013)
37. Zakharov, V.E.: Hamiltonian formalism for hydrodynamic plasma model. Sov. Phys. JETP **33**, 927–932 (1971)
38. Zakharov, V.E.: The Hamiltonian formalism for waves in nonlinear media having dispersion. Radiophys. Quant. Electr. **17**, 326–343 (1974)
39. Gromov, E.M., Malomed, B.A.: Damped solitons in an extended nonlinear Schrödinger equation with a spatial stimulated Raman scattering and decreasing dispersion. Opt. Comm. **320**, 88–93 (2014)
40. Aseeva, N.V., Gromov, E.M., Onosova, I.V., Tyutin, V.V.: Soliton in a higher-order nonlinear Schrödinger equation with spatial stimulated scattering and spatially inhomogeneous second-order dispersion. JETP Lett. **103**, 736–741 (2016)
41. Gromov, E.M., Malomed, B.A., Tyutin, V.V.: Vector solitons in coupled nonlinear Schrödinger equations with spatial stimulated scattering and inhomogeneous dispersion. Commun. Nonlinear Sci. Numer. Simulat. **54**, 13–20 (2018)
42. Gromov, E.M., Malomed, B.A.: Solitons in a forced nonlinear Schrödinger equation with the pseudo-Raman effect. Phys. Rev. E **92**, 062926 (2015)
43. Blit, R., Malomed, B.A.: Propagation and collisions of semidiscrete solitons in arrayed and stacked waveguides. Phys. Rev. A **86**, 043841 (2012)
44. Bogatyrev, V.A., et al.: Single-mode fiber with chromatic dispersion varying along the length. J. Lightwave Tech. **9**, 561–566 (1991)
45. Janssen, P.: The Interaction of Ocean Waves and Wind. Cambridge University Press, Cambridge (2009)
46. Colin, T., Lannes, D.: Long-wave short-wave resonance for nonlinear geometric optics. Duke Math. J. **107**, 351–419 (2001)
47. Duchêne, V.: Asymptotic shallow water models for internal waves in a two-uid system with a free surface. SIAM J. Math. Anal. **42**, 2229–2260 (2010)
48. Craig, W., Guyenne, P., Sulem, C.: Coupling between internal and surface waves. Nat. Hazards **57**, 617–642 (2011)
49. Brunetti, M., Marchiando, N., Berti, N., Kasparian, J.: Nonlinear fast growth of surface gravity waves under the action of wind. Phys. Lett. A **378**, 1025–1030 (2014)
50. Kharif, C., Kraenkel, R.A., Manna, M.A., Thomas, R.: The modulational instability in deep water under the action of wind and dissipation. J. Fluid Mech. **664**, 138–149 (2010)
51. Wahl, R.J., Teague, W.J.: Estimation of Brunt-Väisälä frequency from temperature profiles. J. Phys. Oceanogr. **13**, 2236–2245 (1983)
52. Lifshitz, E.M., Pitaevskii, L.P.: Physical Kinetics. Nauka Publishers, Moscow (1979)
53. Turitsyn, S.K., Schaefer, T., Mezentsev, V.K.: Dispersion-managed solitons. Phys. Rev. E **58**, R5264 (1998)
54. Belanger, P.A., Pare, C.: Dispersion management in optical fiber links: self-consistent solution for the RMS pulse parameters. J. Lightwave Tech. **17**, 445–458 (1999)
55. Pérez-García, V.M., Torres, P.J., Montesinos, G.D.: The method of moments for nonlinear Schrodinger equations: theory and applications. SIAM J. Appl. Math. **67**, 990–1115 (2007)
56. Chen, Z., Taylor, A.J., Efimov, A.: Soliton dynamics in non-uniform fiber tapers: analytical description through an improved moment method. J. Opt. Soc. Am. B **27**, 1022–1030 (2010)